IN VITRO AND IN VIVO CARDIAC TOXICITY OF FLAVORED ELECTRONIC NICOTINE DELIVERY SYSTEMS

Running title: Vaping and cardiac toxicity

Obada Abouassali[1], Mengmeng Chang[1], Bojjibabu Chidipi[1], Jose Luis Martinez[2], Michelle Reiser[1], Manasa Kanithi[1], Ravi Soni[1], Thomas V. McDonald[3], Bengt Herweg[3], Javier Saiz[2], Laurent Calcul[4], Sami F. Noujaim[1,*]

1- Molecular Pharmacology and Physiology, Morsani College of Medicine, University of South Florida, Tampa, USA

2- Ci[2] B, Universitat Politècnica de València, Valencia, Spain

3- Department of Medicine (Division of Cardiology), University of South Florida Morsani College of Medicine, Tampa, FL, United States

4-Department of Chemistry, College of Arts and Sciences, University of South Florida, Tampa, FL, United States

***Correspondence:**

Dr. Sami Noujaim

Molecular Physiology and Pharmacology

Morsani College of Medicine

University of South Florida

12901 Bruce B Downs Blvd

Tampa, FL 33612

Tel: 813 974 6416

e-mail: snoujaim@usf.edu

Keywords:

Vaping, electronic cigarettes, cardiac electrophysiology, arrhythmias

ABSTRACT

The usage of flavored electronic nicotine delivery systems (ENDS) is popular, specifically in the teen and young adult age groups. The possible cardiac toxicity of the flavoring aspect of ENDS is largely unknown. Vaping, a form of electronic nicotine delivery, uses “e-liquid” to generate “e-vapor”, an aerosolized mixture of nicotine and/or flavors. We report our investigation into the cardio-toxic effects of flavored e-liquids. E-vapors containing flavoring aldehydes such as vanillin and cinnamaldehyde, as indicated by mass spectrometry were more toxic in HL-1 cardiomyocytes than fruit flavored e-vapor. Exposure of human induced pluripotent stem cells derived cardiomyocytes to cinnamaldehyde or vanillin flavored e-vapor affected the beating frequency and prolonged the field potential duration of these cells more than fruit flavored e-vapor. Additionally, vanillin aldehyde flavored e-vapor reduced the hERG current in transfected human embryonic kidney cells. In mice, inhalation exposure to vanillin aldehyde flavored e-vapor for 10 weeks caused increased sympathetic predominance in heart rate variability measurements. In vivo inducible ventricular tachycardia was significantly longer, and in optical mapping, the magnitude of ventricular action potential duration alternans was significantly larger in the vanillin aldehyde flavored e-vapor exposed mice compared to control. We conclude that the widely popular flavored ENDS are not harm free, and they have a potential for cardiac harm. More studies are needed to further assess their cardiac safety profile and long- term health effects.

Keywords:

Electronic cigarettes, cardiac electrophysiology, arrhythmias, ENDS

NEW & NOTEWORTHY

The use of electronic nicotine delivery systems (ENDS) is not harm free. It is not known if ENDS negatively affect cardiac electrophysiological function. Our study in cell lines and in mice shows that ENDS can compromise cardiac electrophysiology, leading to action potential instability and inducible ventricular arrhythmias. Further investigations are necessary to assess the long term cardiac safety profile of ENDS products in humans, and to better understand how individual components of ENDS affect cardiac toxicity.

NON- STANDARD ABBREVIATIONS

APJ: Apple jax

APD: Action potential duration

ENDS: Electronic nicotine delivery systems

HF: High frequency

hiPSC: Human induced pluripotent stem cells

HRV: Heart rate variability

GC-MS: Gas chromatography mass spectrometry

LF: Low frequency

MEA: Multiple electrode array

NN: Time separation between consecutive R peaks of the ECG.

pNN06: Percentage of adjacent NN intervals that differ from each other by more than 6 ms.

POG: Hawaiian POG

PSD: Power spectral density

SDNN: Standard deviation of the normal sinus beats.

VC: Vanilla custard

INTRODUCTION

The use of electronic nicotine delivery systems (ENDS) has been growing. It was recently shown that among high school students, ENDS use increased from 1.5% in 2011 to 20.8% in 2018(18). From 2017 to 2018 alone, there was a 75% increase in ENDS use by high school students(18).

The popularity of flavored ENDS likely fueled the proliferation of manufacturers, and the surge in sales of these products(32). In 2014, it was estimated that there were more than 7600 different flavored ENDS products from 466 brands(46), and as of this date, these numbers have only increased. The demand for ENDS continues to grow(44) as evident by a dynamic market(9, 46) which is projected to surpass $6 billion in the next couple of years. However, the health effects and particularly the cardiac toxicity of ENDS remain incompletely understood.

Vaping is a form of electronic nicotine delivery. The vaping device heats the “e-liquid” via a coil in order to generate “e-vapor”, an inhalable smoke-like aerosolized mixture containing nicotine, flavors and solvent particles and their aldehydes . E-liquids are usually a mixture of propylene glycol and vegetable glycerin, flavors, and either nicotine salt or free base nicotine. E-liquids can be used with different ENDS devices such as the pod-based system that requires the use of e-liquid with nicotine salt, or the tank-based vaping system, where a “tank” holds the e-liquid with free base nicotine. Both pod-based and tank-based systems are popular among different age groups(44).

Several studies investigated the toxicity of e-liquids, and it was shown that flavoring aldehydes could be harmful in cell culture(4, 7, 11, 12, 16, 29, 31, 35-38, 43) however, the possible cardiac electrophysiological toxicity of vaping has not been systematically examined and is not completely understood. Here, we will assess the cardiac electrophysiological toxicity

of 3 e-liquids of different flavors, and we will test the hypothesis that vaping can result in cardiac electrophysiological instability and inducible arrhythmogenesis.

MATERIALS AND METHODS

Vaping chamber: A rat housing cage GR900 (width= 34.6 cm, length= 39.5 cm L, and height= 22.7 cm) (Techniplast, Buguggiate, Italy) was modified, where the bottom was fitted for the introduction of the mouthpiece of Smok Species Baby V2, (SMOKTech, Shenzhen, China) vaping device (Figure 1 A). We used the Baby V2 A2 dual sub-coils with a total resistance of 0.2 ohms, at 85 Watts. Inlet and outlet openings were created in the cage's lid. The inlet opening was used to connect the mouthpiece via a plastic tube ¼ ID, 3/8 OD (Fisher Scientific, Waltham, MA) to a flow meter, 1.4 L/ minute, which was connected to a silent fish tank air pump. The outlet opening was fitted with a plastic tube that served as exhaust. A Universal High-powered Door Actuator (ZoneTech, New York, NY)- car door locking mechanism- was fixed alongside the vaping device, aimed at the device's firing button. The actuator was connected to an AC/DC power adapter. Both, the actuator's power adapter and the air pump were wired into the same cycle timer. Every 2 minutes, the cycle timer turns on for 5 seconds. This causes the actuator to push the vaping device's firing button, and simultaneously, air flows into the mouthpiece, expelling, for 4.7 seconds, an e-vapor puff at 1.4 L/ minute inside the cage. The vaping device touch screen displays the duration of the device's activation every time the firing button is pressed. A total of 60 puffs, 110 ml puff volume, over a 2-hour period were delivered. This is consistent with the topography of vaping in ENDS users(8, 17, 23, 34). Figure 1 B is the tank-based vaping device used, and B is a diagram of the exposure system.

Exposure of animals to e-vapor: All animal experiments were approved by the IACUC at the University of South Florida. Ten, 5 months old, C57BL/6J mice (Jackson Laboratory, Bar Harbor, ME) of both sexes were used for air control, and 10 mice (5 months old, of both sexes) were used for vaping exposure. Mice were individually housed in ventilated racks, with ad

libitum access to food and water. For vaping exposure, the ten mice were transferred to the vaping cage, and the mice were simultaneously exposed to 4.7 second puffs of vanilla custard flavored e-vapor at 1.4 L/ minute, every 2 minutes for a total of 60 puffs in a 2-hour period. Mice were exposed 5 days a week, for a period of 10 weeks. Control mice experienced the same handling of the experimental animals. They were placed in a similarly modified chamber, in the same environment, where the only difference was that they were exposed to normal room air. Ten weeks of vaping did not affect the body weight of the animals which was 29.8g ± 0.9 in vaped, and 29.6g ± 0.5 in air control mice.

Preparation of e-vapor extracts: A 10cm x 10cm x 7cm chamber was modified with a bottom opening fitted for the mouthpiece of the Smok Species Baby V2, SMOKTech, vaping device, and inlet and outlet openings were introduced in the chamber's sealing top lid. The inlet tube was connected by plastic tubing into the vaping device's mouthpiece and the flow meter and air pump, as done for the vaping cage above. The outlet was passed through the cap of a 50 ml conical tube containing cell culture media. Another tube was passed into the 50 mL conical tube cap and connected to a liquid trap flask, then to an air flow meter at 1.4 L/ minute, and finally to a vacuum. Similar to the vaping machine, every 2 minutes, the cycle timer turns on for 5 seconds causing the actuator to push the vaping device's firing button; simultaneously, air flows into the mouthpiece, expelling a 4.7 seconds e-vapor puff at 1.4 L/ minute inside the chamber. The resulting puff volume is 110 ml, within the limits of reported ENDS user puff size(34). The vacuum pump draws the e-vapor from the chamber at 1.4 L/ minutes, leading to its bubbling into the medium. 10mL of medium was bubbled with 15 puffs of e-vapor, resulting in an e-vapor concentration of 1.5 puffs per ml of media. For air control, the exact procedure was performed, however, the vaping device was powered off. Dilutions of extracts were

performed with fresh, untreated media. We then tested several concentrations of extracts expressed in puffs/ml as previously done(28). The tested concentrations were 0.075, 0.15, 0.375, and 0.75 puffs/ ml. Figure 1 C is a diagram of the e-vapor extract system.

E-liquids: The flavors used in this study were, Hawaiian POG (POG), and Vanilla Custard (VC) (USA Vape Labs, Huntington Beach, CA), and Apple Jax (APJ) (Epic Juice, Santa Ana, CA). The manufacturer labeled POG flavor as passion fruit, orange and guava, Vanilla Custard, as vanilla custard, and Apple Jax as milky cinnamon apple cereal. These e-liquids are 70% vegetable glycerin/ 30% propylene glycol (70VG/30PG) and are stated by the manufacturer to contain 6mg/ml free base nicotine. We prepared inhouse, base only (70% vegetable glycerin/ 30% propylene glycol) (Sigma-Aldrich) and base plus 6mg/ ml nicotine free base (Sigma-Aldrich).

Total particulate matter measurements: We measured total particulate matter (TPM) generated from the 3 different e-liquids using a 25 mm membrane filter (PALL Life Science) placed into a stainless-steel filter holder (Cole-Parmer). E-vapor was generated using the same method and setup used to bubble cell culture medium, but instead of bubbling the vapor in the medium, the 15 puffs were passed through the filter paper. Filter papers were weighed before and after the procedure.

HL1 cell culture: HL-1 cells (mouse atrial myocytes) were obtained from the laboratory of Dr. Claycomb (Louisiana State University) and cultured following the recommended protocol(5). Briefly, cells were grown in Claycomb medium (Sigma, St. Louis, MO) and supplemented with 10% FBS (Sigma, St. Louis, MO), 0.1 mM norepinephrine (Sigma, St. Louis, MO), 2mM L-Glutamine (Sigma, St. Louis, MO), and penicillin/streptomycin (100U/ml/100µ/mL) on tissue culture plates (Corning, Corning, NY), coated with fibronectin/gelatin (Sigma, St. Louis, MO).

Apoptosis flow cytometry: Apoptosis was measured using the FITC annexin V staining assay (BD, Franklin Lakes, NJ). HL-1 cells were plated in 12 well plates, and when confluency reached approximately 70%, they were cultured with control medium, or with e-vapor extracts. The tested concentrations were 0.075, 0.15, 0.375, and 0.75 puffs/ml, and the duration of exposure was 24 or 48 hours. After the incubation period, the cells in each well were lifted with Accutase and re-suspended in 5 mL PBS. Cells were pelleted by centrifugation, washed with PBS and stained with FITC labeled annexin V according to the manufacturer's recommendation. DAPI (3 μM) was added immediately before reading the samples on a BD LSRII Cytometer using the 488-nm and 405-nm lasers for excitation of FITC annexin V and DAPI respectively. The following controls are included in each experiment: unstained cells, cells stained with FITC annexin V, but not with DAPI, and cells stained with DAPI, but not with FITC annexin V. Data analysis was carried out using the FlowJo software.

Human induced pluripotent stem cells derived cardiomyocytes (hiPSC) culture and extracellular potentials recording: The iCell Cardiomyocytes2 (Cellular Dynamics, Madison, WI) were thawed according to the manufacturer's protocol, and 50,000 cells/well were plated on the fibronectin (50 μg/ml) coated 24 wells multiple electrode array (MEA) plates (24well plate-eco), (MED64, Osaka, Japan). Plated cells were incubated at 37°C, 5% CO2 for one hour to allow attachment of the cells, after which, pre-warmed maintenance medium (Cellular Dynamics, Madison, WI) was added to the wells. The maintenance medium was changed every three days, and after day 7, cells began to beat synchronously, periodically and spontaneously. The Presto Multielectrode Array (MED64, Osaka, Japan) was used to record extracellular potentials of the spontaneously beating hiPSC derived cardiomyocytes. The Presto is equipped with an environmental chamber (37°C and 95% O2/ 5% CO2). After the

plate was placed on top of the recording electrodes, 2-minute recordings of the extracellular potentials were obtained using the MED64's MEA Symphony software interface at baseline before addition of the vapor extracts, and after addition of the extracts. For each well, the beating rate, and the Bazett corrected field potential durations were calculated in the MED64's MEA Symphony analysis software.

Patch clamp: Human embryonic kidney (HEK 293) cells were co- transfected with wild type hERG and GFP in pcDNA3. 48h post-transfection, cells were cultured with 0.375 puffs/ml vanilla custard e-vapor or with air control. The hERG current (I_{Kr}) was measured by whole-cell configuration as usually done(1), using an Axon 700B amplifier and (Digidata 1550B A/D converter). The bath solution contained 140 mM NaCl, 2 mM $CaCl_2$, 4 mM KCl, 1 mM $MgCl_2$, 5 mM glucose, and 10 mM HEPES buffer (pH 7.4). The internal solution contained 126 mM KCl, 4 mM Mg-ATP, 2 mM $MgSO_4$, 5 mM EGTA, 0.5 mM $CaCl_2$, and 25 mM HEPES buffer (pH 7.2). Voltage protocol: 10 mV steps from -60 to 60 mV for 3 s, then step to - 40 mV for 1 s, and finally hyperpolarized to -120 mV for 0.5 s. Tail current amplitude was quantified and normalized to cell capacitance (nA/pF) and presented in an IV curve.

Mass spectrometry: E-vapors were generated using the same setup described in Figure 1. The 10cm x 10cm x 7cm chamber was slightly altered, where the outlet tube was replaced with a septum. 5 puffs were generated, each for 4.7s at an interval of 10s, at a flow rate of 1.4 L/min. Immediately after the smoke was generated, a 2.5mL Hamilton glass tight syringe was introduced through the septum to extract 250 µL of e-vapor from the chamber. The smoke was then immediately injected manually into the Aglient 7890B gas chromatography, mass spectrometer (GC-MS) 5977B. The headspace syringe was cleaned between samples by rinsing repeatedly in pesticide grade methanol and then thoroughly dried in an incubator for 30

mins at 70ºC. The GC-MS parameters were optimized based on previous studies(10, 37) and are reported in Table 1. MassHunter Workstation Qualitative Analysis Software (Version B.07.00 SP2) in conjunction with NIST MS Search 2017 Library were used for analysis. Peaks were identified based on a match score factor higher than 700.

Telemetry and HRV analysis: Mice were implanted with ECG telemetric devices (ETA-F10, Data Sciences International, St. Paul, MN) using sterile equipment, under general anesthesia with 2% Isoflurane, and body temperature maintained at 37°C on a heating pad. The manufacturer's recommendation for subcutaneous transmitter placement along the lateral flank was followed. The animals were allowed to recover for fourteen days after the implantation procedure. ECG recordings in freely moving animals were done using the PhysioTel RPC-3 (Data Sciences International, St. Paul, MN) receivers, after 1, 5, or 10 weeks of exposure to vanilla custard e-vapor. The ECGs were recorded using the Ponemah Software (Data Sciences International, St. Paul, MN), at 1kHz sampling rate, about 4 hours after conclusion of the vaping session, in order to allow the animals to settle in their cages, after handling and exposure. Thirty minutes ECG strips were prepared and analyzed in MatLab. Pan-Tompkins algorithm was used to extract the time separation between consecutive R peaks of the ECG. R-R values not contained between mean R–R interval +/- 2 standard deviation were inspected for arrhythmias (no arrhythmias were observed) and excluded in order to obtain normal R-R intervals (NN intervals) (33, 41). Parametrization of HRV was performed in LabView (National Instruments) as previously done (33, 41). Two temporal and two spectral parameters were subsequently further analyzed. The temporal parameters were standard deviation of the normal sinus rhythm beats (SDNN) and the percentage of adjacent NN intervals that differ from each other by more than 6 milliseconds (pNN06). pNN is an indicator of cardiac

parasympathetic activity (39, 41) which in humans is usually 50 ms, but was adapted to 6 ms in mouse studies due to the high heart rate of the mouse (41). Spectral parameters were calculated from the unmodified periodogram as an estimator of the power spectral density (PSD). Low frequency was defined as 0.15 Hz to 1.5 Hz, and high frequency as 1.5 Hz to 5 Hz, similarly to what is done in mouse HRV studies (33, 39, 41).

In vivo VT inducibility: Mice were anesthetized (2% isofluorane), and a 1.2 French octapolar catheter (Millar, Houston, TX) was placed transvenously into the right atrium, and advanced into the right ventricle. Electrograms were recorded using the PowerLab platform (AD Instruments, Colorado Springs, CO). Programmed electrical stimulation for VT induction was performed by pacing the right ventricle at twice diastolic threshold with 1 second bursts from 20 to 50 Hz, in 2 Hz increments(14, 33).

Optical imaging: Isolated Langendorf perfused mouse hearts were retrogradely perfused with Tyrode's solution. The preparations were maintained at 37°C and stained with a bolus of voltage sensitive dye (0.25 ml, 10 μM Di 4 ANEPPS, Sigma, St. Louis, MO). Blebbistatin (7 μM, Sigma, St. Louis, MO) was used as an excitation-contraction uncoupler. Mapping was carried out as we have done extensively. We quantified the action potential duration at 75% repolarization (APD) as we previously did(30, 45). A bipolar, silver tip stimulation electrode was used to pace the ventricles (5ms pulses, 2x diastolic threshold) at different frequencies (from 8 to 15 Hz).

Statistics: Data are presented as average ± standard error. Student's t-test, one way analysis of variance (ANOVA) with Bonferroni correction were used as appropriate and significance was taken at $p<0.05$.

RESULTS

HL-1 mouse atrial cardiomyocytes(5) were cultured for 48 h with air or with 0.075, 0.15, 0.375, and 0.75 puffs/ml vanilla custard (USA Vape Lab, CA) e-vapor extract. Cells were then dissociated with Accutase and stained with FITC labeled annexin V, a widely used apoptotic marker, and DAPI, a cell viability marker. Figure 2 A, left panel, shows a flow cytometry analysis of air controls. The majority of cells are in the low annexin V and low DAPI live quadrant. Apoptotic cells show high annexin V (right lower and upper quadrants). Necrotic cells show low annexin V and high DAPI labeling. In vanilla custard e-vapor treatment, there was a significant shift of the population from the live quadrant, to the necrotic and apoptotic quadrants. Panel B quantifies the percentage of live cells at 0.075, 0.15, 0.375, and 0.75 puffs/ml treatment with air, or vanilla custard e-vapor. There was a dose dependent decrease in the live population as the concentration of vanilla custard e-vapor increased. The percentage of necrotic (panel C) and apoptotic (panel D) cells increased with increasing vanilla custard e-vapor extract. Panel E is a plot of the toxicity index (TI) which we calculated as $TI = \frac{\%\,DC + \%\,AC}{\%\,LC}$ where %DC is the percentage of dead cells, %AC is the percentage of apoptotic cells, and %LC is the percentage of live cells per well. The TI was normalized to that of air at each treatment condition. Figure 2E is the TI normalized to that of air at 0.075, 0.15, 0.375, and 0.75 puffs/ml vanilla custard extract, where TI was 1.3 ± 0.04, 1.4 ± 0.03, 4.3 ± 0.13, and 13.6 ± 3.5 respectively.

Figure 3A compares the effects of 48 h, 0.75 puffs/ml e-vapor extracts of Hawaiian POG (POG), vanilla custard (VC) and apple jax (APJ) or air on HL-1 myocytes. Flow cytometry of

annexin V and DAPI staining showed that all three e-liquids decreased viability (top panel) and increased apoptosis (middle panel) to different extents (*p<0.01, vs air). The bottom panel shows that VC and APJ were more toxic compared to POG (*p<0.01), where the respective toxicities were 22.7 ± 1.75, 185 ± 29.9, and 1.53 ± 0.09. 24h exposures resulted in lower toxicities compared to 48h, and the respective toxicities of VC, APJ, and POG at 24h were 8.9 ± 2.2, 5.3 ± 0.8 and 2.3± 0.6.

We measured the total particulate matter (TPM) generated from the 3 different e-liquids. TPM measurements were not different between the 3 e-liquids. For vanilla custard, apple jax, and POG, the measured respective TPM values were 2.74 mg/puff ± 0.075, 2.67 mg/puff ± 0.060, and 2.66 mg/puff ± 0.067, n=3 each.

We then used gas GC-MS to analyze the chemical composition of these e-liquids. Figure 3 B shows the total ion chromatograms of vanilla custard (VC), apple jax (APJ) and POG. The complete list of identified constituents in these e-liquids is presented in Table 2. The propylene glycol, glycerin, and nicotine peaks are evident(37),(10). In vanilla custard and apple jax, but not in POG, flavorings peaks corresponding to aldehydes products such as cinnamaldehyde, vanillin, and ethyl vanillin (black arrows) are present. This is consistent with cell culture studies, showing that vanilla, and cinnamon containing flavors cause higher toxicities(37), however, in non-cardiomyocyte cell lines were used(37). Here we show that in a cardiac myocyte cell line, vanilla and cinnamon flavored e-liquids also cause higher toxicities compared to fruit flavored e-liquids.

Next, we tested in spontaneously beating hiPSC derived cardiomyocytes, the effects of the 3 e-liquids on beating rate and corrected field potential durations. hiPSC cardiomyocytes were seeded in 24 well MEA plates. Each well contained 16 electrodes in a 4x4 configuration, 100

μm interelectrode distance. The Presto Multielectrode Array was used to simultaneously record the 16 unipolar extracellular potentials in each well. Only wells that showed spontaneous activity were used. 48 h exposure to the e-vapors at 0.75 puffs/ml was deadly to the cells. We thus reduced the exposure duration and concentration. At 24 h, and 0.15 puffs/ml, VC and APJ reduced the beating rate (Figure 4A) and prolonged the corrected field potential duration (FPD) (Figure 4B) more significantly than POG (*$p<0.05$ vs air, and $^{\#}p<0.05$ vs VC and APJ). We then conducted a series of experiments comparing the effects of 0.15 puffs/ml of base only (70VG/30PG), base with nicotine (70VG/30PG plus 6mg/ml nicotine base), and vanilla custard e-liquid (stated by manufacturer to contain 6mg/ml nicotine free base) on beating rate and on the field potential duration in hiPSC derived cardiomyocytes. Our results showed that base only had no significant effects on the beating rate or the FPD versus air control (Figure 4C, first 2 traces, and Figures 4D and E). Base with 6mg/ml nicotine (Base+Nic) significantly decreased the beating rate and tended to increase the FPD versus control (Figure 4C third trace, and Figures 4D and E) and vanilla custard (base plus 6mg/ml nicotine plus flavorings) further decreased the beating rate and further increased the FPD (Figure 4C fourth trace, and Figures 4D and E) (*$p<0.05$ vs air, and $^{\#}p<0.05$ vs Base+Nic). This experiment suggested that flavorings in vanilla custard increased the toxicity of base with nicotine. We then tested a higher concentration of vanilla custard (0.375 puffs/ml). 7 of 10 treated wells stopped beating, while the 3 remaining cells showed tachycardia like activity (74.5 beats per minute $\pm$ 12.3 versus 39 beats per minute $\pm$ 3 at baseline, $p<0.05$). The last trace of Figure 4C shows such tachycardic activity. The prolongation of the FPD suggested that vaping could affect ion channels including the hERG current (I_{Kr}). It has been shown in hiPSC cardiomyocytes that I_{Kr} block reduces beating rate and increases field potential duration(24). Additionally, block of I_{Kr}

can lead to tachyarrhythmias. Thus, we investigated whether the I_{Kr} current is affected by vanilla custard flavored e-vapor and we assessed the effects of 0.375 puffs/ml vanilla custard e-vapor on I_{Kr} in HEK293 cells transfected with hERG. In Figure 5 A, 24 hours treatment with vanilla custard e-vapor caused a reduction in the currents elicited in response to voltage steps from -60 to +60mV compared to control. In B, the IV relationship of the tail currents indicated that vanilla custard e-vapor significantly inhibited I_{Kr} (*$p<0.01$, air control vs VC, t-test). As a whole, this set of experiments suggested that flavorings increase the toxicity of base with nicotine, and that vaping can affect the human cardiac electrophysiology in part through possible modulation of I_{Kr}.

Next, we investigated the effects of 10 weeks inhalation exposure to vanilla custard e-vapor, an e-liquid with high toxicity (Figures 3 and 4) versus air, on heart rate variability parameters in mice instrumented with telemetric ECG. HRV parameters were measured at baseline, 1, 5, and 10 weeks exposure. Figure 6A shows the histograms of successive differences in NN. The left graph is from an air control mouse. There were no differences between the histograms at baseline (blue trace) and at week 10 (orange trace) of air exposure. The right graph is from a vaped mouse, and shows less variation in successive NN differences after 10 weeks of vaping (orange histogram) compared to baseline (blue histogram). The dashed lines indicate the marks for 6 ms increase or decrease in successive NN differences.

The histograms were then used to calculate SDNN, which was not different in mice exposed to air (black circles) versus vaped mice (gray circles) at 0, 1, 5, and 10 weeks (Figure 6B, left panel). Another temporal HRV parameter that computes the percentage of adjacent NN intervals that differ from each other by more than 6 ms (pNN06) was investigated (Figure 6B, right panel). There were no statistically significant differences in pNN06 in mice exposed to

air (black circles) versus vaped mice (gray circles) at 0, and 1 week. However, pNN06 was significantly decreased in vape versus air at 5 and 10 weeks (*$p<0.05$, vape versus air, 5 weeks. #$p<0.05$, vape versus air, 10 weeks). pNN is an indicator of cardiac parasympathetic activity (39, 41) which in humans is usually 50 ms, but 6 ms was used in mouse studies due to the high heart rate of the mouse(41). These data suggest that vaping decreased cardiac parasympathetic activity leading to a sympathetic predominance, and thus sympathovagal disbalance.

Spectral analysis was also carried out. Figure 6C shows periodograms as estimators of the PSD. PSD from a mouse exposed to air (left graph) is similar at baseline (blue line) and after 10 weeks (orange line). The PSD from a vaped mouse (right graph) shows a visible decrease in the high frequency band after 10 weeks of exposure to e-vapor. Quantification of the spectral HRV parameters (low frequency; LF and high frequency; HF), are shown in panel D. The LF component did not significantly change, however, HF was significantly lower in vape versus air at 5 and 10 weeks (*$p<0.05$, vape versus air, 5 weeks. #$p<0.05$, vape versus air, 10 weeks). The reduction in HF parallels the finding in the temporal analysis, which showed reduction in pNN06 in vaped mice. This is not surprising since both of these parameters are correlated(39, 41). Furthermore, HRV changes in vaped mice are consistent with what has been shown in human subjects who are habitual electronic cigarette users (26) as well as in the setting of acute use(25). Such changes in HRV due to vaping, are indicative of possible sympathovagal disbalance in the control of heart rate, which is clinically linked to poor cardiovascular outcomes(6, 39).

We studied the in vivo inducibility of VT in 5 wild type mice exposed to vaping with vanilla custard for 10 weeks versus 7 mice exposed to air control, using in vivo programmed

electrical stimulation. The ECGs of Figure 7 show that a 1 second, 36 Hz burst stimulus at 1 mA, induced a short-lived ventricular tachycardia (VT) episode, after which the heart reverted back to sinus rhythm. In the vaped mouse, a similar burst stimulus induced a longer VT episode. Six out of 7 air control mice had VT, while 5 out of 5 vaped animals had VT, however, as shown in the bar graph, the duration of VT episodes was significantly longer in vaped compared to WT mice (t-test, $p<0.05$).

Subsequently, in 4 air control and 3 vaped mice we conducted epicardial optical mapping of voltage. Figure 8 panels A and B show maps of action potential duration at 75% repolarization (APD_{75}) of the anterior surface of the ventricles at 10 and 15 Hz pacing respectively. Pacing was done from the apex as indicated by the white stair symbol. RV and LV are the right and left ventricles. In A, the top maps are representatives of paced beat 1, and the middle maps are representatives of the subsequent paced beat 2 in control and vaped hearts. Single-pixel recordings of the action potentials are underneath the top maps, and they show beat 1 and beat 2. The action potential duration was not different between beat 1, and the subsequent beat 2, as evidenced by the difference map in the bottom (map 1 minus map 2). In panel B, the hearts were paced at 15 Hz. It can be appreciated from the single pixel recordings of the optical action potential, and from the APD maps, that while in control the APD did not change considerably between beat 1 and 2, action potential duration alternans occurred in the vaped heart, where one beat is long (beat 1), while the successive beat is short (beat 2). These APD alternans can be visualized in the difference map (bottom). Panel C plots the averaged action potential durations in 4 control hearts, quantified from the APD maps at different pacing frequencies (from 8 to 15 Hz). No significant alternans occurred. Panel D is the averaged action potential durations in 3 vaped hearts, paced from 8 to 15 Hz. Significant

alternans occurred at 15 Hz (*p<0,01, t-test), indicating that vaping induces action potential changes in the heart. It has been shown that alternans are indicators of cardiac electrophysiological instability and could lead to arrhythmogenesis(42).

DISCUSSION

Flavored ENDS are very popular, and it has been argued that the appeal of flavored ENDS products has fueled the rapid and spectacular growth of this industry(9, 46). Thus, our objective was to investigate the in vitro and in vivo cardiac electrophysiological toxicity of flavorings in ENDS. Our study showed that exposure to ENDS aerosols could result in cellular and whole organ electrophysiological toxicity that includes action potential instability and reduction in heart rate variability parameters. Therefore, it is possible that ENDS are not harm free to the electrophysiological function of the heart.

In HL-1 mouse atrial cardiomyocytes(5) the 3 e-liquids tested were toxic, however to different extents. Aldehyde containing vanilla custard and apple jax flavors, as determined by GC-MS, were more detrimental compared to the fruity flavored e-liquid. This is independent of nicotine content, since these e-liquids are stated to contain 6 mg/ml nicotine. These findings are consistent with similar studies conducted in many other cell lines, however, these cell lines are not relevant to cardiac electrophysiology(11, 29, 31, 36-38). In spontaneously beating hiPSC derived cardiomyocytes, e-vapor affected the beating rate , prolonged the corrected field potential duration (a surrogate for the QTc interval)(22), and inhibited I_{Kr}. This raises the possibility that vaping could be arrhythmogenic since in the heart, prolongation of the QT interval is associated with the development of fast ventricular rhythms that include tachycardia and fibrillation(2).

HRV analysis revealed patterns of change indicative of sympathovagal disbalance in the control of the mouse heart due to exposure to ENDS aerosols where temporal and spectral indices of parasympathetic modulation of heart rate variability were decreased. These changes are consistent with what has been shown in human subjects who are habitual electronic cigarette users (26) as well as in the setting of acute electronic cigarette use(25). It is generally accepted that in HRV measurements, sympathovagal disbalance could correlate with the development of arrhythmias and poor cardiovascular outcome(6, 39). This is in line with the in vivo VT inducibility studies which we conducted, where in vaped mice, inducible VT was more sustained compared to air control mice, and where in optical mapping, vaping resulted in action potential instability which manifested as action potential alternans. It has been shown in human subjects that the use of electronic cigarettes with nicotine affected repolarization indices on the ECG(13), and in mice, it was shown that ENDS constituents including vegetable glycerin caused prolongation of the QT interval(3).

In conclusion, our study suggests that exposure to ENDS aerosols could result in cardiac electrophysiological toxicity that includes prolongation of repolarization, hERG block, sympathovagal disbalance, inducibility of VT, and action potential alternans. The respiratory system is the major route of ENDS smoke entry into the body, and vaping related pulmonary illnesses are increasingly documented in the clinic(27). However, similarly to combustible tobacco smoking, ENDS use could have potentially harmful effects on the heart. Our work demonstrates that vaping compromises the cardiac electrophysiological integrity, and further studies are needed to further assess the long-term cardiac safety profile of ENDS products.

LIMITATIONS:

Our results in the mouse hearts suggested that vaping can lead to inducible ventricular tachyarrhythmias. Other than a case report that attributed the occurrence of atrial fibrillation to vaping in an otherwise healthy teen(21), arrhythmias have not yet been directly linked to the use of ENDS in the young population. Therefore, caution should be exercised when extrapolating the findings in the mouse heart to the human heart due to the presence of many obvious differences including those related to important species differences in the ionic bases of the action potential(15). In the in-vitro experiments, we do not know if the concentrations of ENDS constituents in the bubbled media are similar to those that could actually reach the heart through inhalation exposure to ENDS aerosols. When generating the e-vapor, the full impact of reversing airflow through the mouthpiece is unknown. Plasma or urine nicotine levels were not measured in the vaped mice. HRV measurements were performed 4 hours after vaping. The reported nicotine half- life in C57BL/6 mice is about 9 minutes(40). Studies have shown that the manufacturer stated nicotine levels in some ENDS products have been inaccurate(20). The stated nicotine level of 6mg/ml in the e-liquids we used are not verified, and are reported in this manuscript, as printed on the products' labels. Additionally, it is not inconceivable that that there may be contaminants(19) or variable grades of nicotine and/or solvents used by different companies. Such possible confounders have not been tested in this work. Further investigations are necessary to assess the long- term cardiac safety profile of ENDS products in humans, and to better understand how individual components of ENDS affect cardiac toxicity.

ACKNOWLEDGEMENTS:

This work was supported in part by National Institutes of Health grants R21HL138064, and R01HL129136 to SN, and AHA postdoctoral fellowship to BC.

REFERENCES

1. **Bertalovitz AC, Badhey MLO, and McDonald TV**. Synonymous nucleotide modification of the KCNH2 gene affects both mRNA characteristics and translation of the encoded hERG ion channel. *J Biol Chem* 293: 12120-12136, 2018.
2. **Bertino JS, Jr., Owens RC, Jr., Carnes TD, and Iannini PB**. Gatifloxacin-associated corrected QT interval prolongation, torsades de pointes, and ventricular fibrillation in patients with known risk factors. *Clinical infectious diseases : an official publication of the Infectious Diseases Society of America* 34: 861-863, 2002.
3. **Carll A, Salatini R, Arab C, Holbrook D, Bhatnagar A, and Conklin D**. Electronic Cigarette Aerosols and Constituents Induce Bradycardia and Prolonged QT in Mice -- Does E-Cigarette Use Increase Cardiovascular Disease Risk? *Circulation* 136: A20454, 2017.
4. **Cervellati F, Muresan XM, Sticozzi C, Gambari R, Montagner G, Forman HJ, Torricelli C, Maioli E, and Valacchi G**. Comparative effects between electronic and cigarette smoke in human keratinocytes and epithelial lung cells. *Toxicology in vitro : an international journal published in association with BIBRA* 28: 999-1005, 2014.
5. **Claycomb WC, Lanson NA, Jr., Stallworth BS, Egeland DB, Delcarpio JB, Bahinski A, and Izzo NJ, Jr.** HL-1 cells: a cardiac muscle cell line that contracts and retains phenotypic characteristics of the adult cardiomyocyte. *Proceedings of the National Academy of Sciences of the United States of America* 95: 2979-2984, 1998.
6. **Colhoun HM, Francis DP, Rubens MB, Underwood SR, and Fuller JH**. The association of heart-rate variability with cardiovascular risk factors and coronary artery calcification: a study in type 1 diabetic patients and the general population. *Diabetes care* 24: 1108-1114, 2001.
7. **Crotty Alexander LE, Drummond CA, Hepokoski M, Mathew D, Moshensky A, Willeford A, Das S, Singh P, Yong Z, Lee JH, Vega K, Du A, Shin J, Javier C, Tian J, Brown JH, and Breen EC**. Chronic inhalation of e-cigarette vapor containing nicotine disrupts airway barrier function and induces systemic inflammation and multiorgan fibrosis in mice. *American journal of physiology Regulatory, integrative and comparative physiology* 314: R834-R847, 2018.
8. **Cunningham A, Slayford S, Vas C, Gee J, Costigan S, and Prasad K**. Development, validation and application of a device to measure e-cigarette users' puffing topography. *Scientific reports* 6: 35071, 2016.

9. **Day HR, Ambrose BK, Schroeder MJ, and Corey CG**. Point of Sale Scanner Data for Rapid Surveillance of the E-cigarette Market. *Tobacco regulatory science* 3: 325-332, 2017.
10. **Eddingsaas N, Pagano T, Cummings C, Rahman I, Robinson R, and Hensel E**. Qualitative Analysis of E-Liquid Emissions as a Function of Flavor Additives Using Two Aerosol Capture Methods. *International journal of environmental research and public health* 15: 2018.
11. **Farsalinos KE, Romagna G, Allifranchini E, Ripamonti E, Bocchietto E, Todeschi S, Tsiapras D, Kyrzopoulos S, and Voudris V**. Comparison of the cytotoxic potential of cigarette smoke and electronic cigarette vapour extract on cultured myocardial cells. *International journal of environmental research and public health* 10: 5146-5162, 2013.
12. **Hwang JH, Lyes M, Sladewski K, Enany S, McEachern E, Mathew DP, Das S, Moshensky A, Bapat S, Pride DT, Ongkeko WM, and Crotty Alexander LE**. Electronic cigarette inhalation alters innate immunity and airway cytokines while increasing the virulence of colonizing bacteria. *Journal of molecular medicine* 94: 667-679, 2016.
13. **Ip M, Diamantakos E, Haptonstall K, Choroomi Y, Moheimani RS, Nguyen KH, Tran E, Gornbein J, and Middlekauff HR**. Tobacco and electronic cigarettes adversely impact ECG indexes of ventricular repolarization: implication for sudden death risk. *American journal of physiology Heart and circulatory physiology* 318: H1176-H1184, 2020.
14. **Jin H, Welzig CM, Aronovitz M, Noubary F, Blanton R, Wang B, Rajab M, Albano A, Link MS, Noujaim SF, Park HJ, and Galper JB**. QRS/T-wave and calcium alternans in a type I diabetic mouse model for spontaneous postmyocardial infarction ventricular tachycardia: A mechanism for the antiarrhythmic effect of statins. *Heart rhythm* 14: 1406-1416, 2017.
15. **Kaese S, and Verheule S**. Cardiac electrophysiology in mice: a matter of size. *Frontiers in physiology* 3: 345, 2012.
16. **Khlystov A, and Samburova V**. Flavoring Compounds Dominate Toxic Aldehyde Production during E-Cigarette Vaping. *Environmental science & technology* 50: 13080-13085, 2016.
17. **Kosmider L, Jackson A, Leigh N, O'Connor R, and Goniewicz ML**. Circadian Puffing Behavior and Topography Among E-cigarette Users. *Tobacco regulatory science* 4: 41-49, 2018.
18. **Kuehn B**. Youth e-Cigarette Use. *Jama* 321: 138, 2019.
19. **Lee MS, Allen JG, and Christiani DC**. Endotoxin and [Formula: see text] Contamination in Electronic Cigarette Products Sold in the United States. *Environmental health perspectives* 127: 47008, 2019.
20. **Lisko JG, Tran H, Stanfill SB, Blount BC, and Watson CH**. Chemical Composition and Evaluation of Nicotine, Tobacco Alkaloids, pH, and Selected Flavors in E-Cigarette Cartridges and Refill Solutions. *Nicotine & tobacco research : official journal of the Society for Research on Nicotine and Tobacco* 17: 1270-1278, 2015.
21. **Lowe R, Klingaman C, Golten A, and Davis T**. Atrial fibrillation with e-cigarette use in an otherwise healthy adolescent male. *Pediatrics* 146: 312-313, 2020.
22. **Iuerman G, Obejero-Paz C, Brown A, and Bruening-Wright A**. Optimizing Rate Correction of Field Potential Duration, a Biomarker for QT Risk Assessment, in Human Ipsc-Cardiomyocytes. *Biophysical J* 106: 720, 2014.
23. **Mikheev VB, Buehler SS, Brinkman MC, Granville CA, Lane TE, Ivanov A, Cross KM, and Clark PI**. The application of commercially available mobile cigarette topography

devices for e-cigarette vaping behavior measurements. *Nicotine & tobacco research : official journal of the Society for Research on Nicotine and Tobacco* 2018.
24. **Millard D, Dang Q, Shi H, Zhang X, Strock C, Kraushaar U, Zeng H, Levesque P, Lu HR, Guillon JM, Wu JC, Li Y, Luerman G, Anson B, Guo L, Clements M, Abassi YA, Ross J, Pierson J, and Gintant G**. Cross-Site Reliability of Human Induced Pluripotent stem cell-derived Cardiomyocyte Based Safety Assays Using Microelectrode Arrays: Results from a Blinded CiPA Pilot Study. *Toxicological sciences : an official journal of the Society of Toxicology* 164: 550-562, 2018.
25. **Moheimani RS, Bhetraratana M, Peters KM, Yang BK, Yin F, Gornbein J, Araujo JA, and Middlekauff HR**. Sympathomimetic Effects of Acute E-Cigarette Use: Role of Nicotine and Non-Nicotine Constituents. *Journal of the American Heart Association* 6: 2017.
26. **Moheimani RS, Bhetraratana M, Yin F, Peters KM, Gornbein J, Araujo JA, and Middlekauff HR**. Increased Cardiac Sympathetic Activity and Oxidative Stress in Habitual Electronic Cigarette Users: Implications for Cardiovascular Risk. *JAMA cardiology* 2: 278-284, 2017.
27. **Mukhopadhyay S, Mehrad M, Dammert P, Arrossi AV, Sarda R, Brenner DS, Maldonado F, Choi H, and Ghobrial M**. Lung Biopsy Findings in Severe Pulmonary Illness Associated With E-Cigarette Use (Vaping). *Am J Clin Pathol* 2019.
28. **Munakata S, Ishimori K, Kitamura N, Ishikawa S, Takanami Y, and Ito S**. Oxidative stress responses in human bronchial epithelial cells exposed to cigarette smoke and vapor from tobacco- and nicotine-containing products. *Regulatory toxicology and pharmacology : RTP* 99: 122-128, 2018.
29. **Muthumalage T, Prinz M, Ansah KO, Gerloff J, Sundar IK, and Rahman I**. Inflammatory and Oxidative Responses Induced by Exposure to Commonly Used e-Cigarette Flavoring Chemicals and Flavored e-Liquids without Nicotine. *Frontiers in physiology* 8: 1130, 2017.
30. **Noujaim SF, Kaur K, Milstein M, Jones JM, Furspan P, Jiang D, Auerbach DS, Herron T, Meisler MH, and Jalife J**. A null mutation of the neuronal sodium channel NaV1.6 disrupts action potential propagation and excitation-contraction coupling in the mouse heart. *FASEB J* 26: 63-72, 2012.
31. **Palpant NJ, Hofsteen P, Pabon L, Reinecke H, and Murry CE**. Cardiac development in zebrafish and human embryonic stem cells is inhibited by exposure to tobacco cigarettes and e-cigarettes. *PloS one* 10: e0126259, 2015.
32. **Prochaska JJ**. The public health consequences of e-cigarettes: a review by the National Academies of Sciences. A call for more research, a need for regulatory action. *Addiction* 114: 587-589, 2019.
33. **Rajab M, Jin H, Welzig CM, Albano A, Aronovitz M, Zhang Y, Park HJ, Link MS, Noujaim SF, and Galper JB**. Increased inducibility of ventricular tachycardia and decreased heart rate variability in a mouse model for type 1 diabetes: effect of pravastatin. *American journal of physiology Heart and circulatory physiology* 305: H1807-1816, 2013.
34. **Robinson RJ, Hensel EC, Roundtree KA, Difrancesco AG, Nonnemaker JM, and Lee YO**. Week Long Topography Study of Young Adults Using Electronic Cigarettes in Their Natural Environment. *PloS one* 11: e0164038, 2016.
35. **Rowell TR, Reeber SL, Lee SL, Harris RA, Nethery RC, Herring AH, Glish GL, and Tarran R**. Flavored e-cigarette liquids reduce proliferation and viability in the CALU3 airway

epithelial cell line. *American journal of physiology Lung cellular and molecular physiology* 313: L52-L66, 2017.
36. **Sancilio S, Gallorini M, Cataldi A, and di Giacomo V**. Cytotoxicity and apoptosis induction by e-cigarette fluids in human gingival fibroblasts. *Clinical oral investigations* 20: 477-483, 2016.
37. **Sassano MF, Davis ES, Keating JE, Zorn BT, Kochar TK, Wolfgang MC, Glish GL, and Tarran R**. Evaluation of e-liquid toxicity using an open-source high-throughput screening assay. *PLoS biology* 16: e2003904, 2018.
38. **Scheffler S, Dieken H, Krischenowski O, Forster C, Branscheid D, and Aufderheide M**. Evaluation of E-cigarette liquid vapor and mainstream cigarette smoke after direct exposure of primary human bronchial epithelial cells. *International journal of environmental research and public health* 12: 3915-3925, 2015.
39. **Shaffer F, and Ginsberg JP**. An Overview of Heart Rate Variability Metrics and Norms. *Frontiers in public health* 5: 258, 2017.
40. **Siu EC, and Tyndale RF**. Characterization and comparison of nicotine and cotinine metabolism in vitro and in vivo in DBA/2 and C57BL/6 mice. *Mol Pharmacol* 71: 826-834, 2007.
41. **Thireau J, Zhang BL, Poisson D, and Babuty D**. Heart rate variability in mice: a theoretical and practical guide. *Exp Physiol* 93: 83-94, 2008.
42. **Tse G, Wong ST, Tse V, Lee YT, Lin HY, and Yeo JM**. Cardiac dynamics: Alternans and arrhythmogenesis. *J Arrhythm* 32: 411-417, 2016.
43. **Yu V, Rahimy M, Korrapati A, Xuan Y, Zou AE, Krishnan AR, Tsui T, Aguilera JA, Advani S, Crotty Alexander LE, Brumund KT, Wang-Rodriguez J, and Ongkeko WM**. Electronic cigarettes induce DNA strand breaks and cell death independently of nicotine in cell lines. *Oral oncology* 52: 58-65, 2016.
44. **Zare S, Nemati M, and Zheng Y**. A systematic review of consumer preference for e-cigarette attributes: Flavor, nicotine strength, and type. *PloS one* 13: e0194145, 2018.
45. **Zarzoso M, Rysevaite K, Milstein ML, Calvo CJ, Kean AC, Atienza F, Pauza DH, Jalife J, and Noujaim SF**. Nerves projecting from the intrinsic cardiac ganglia of the pulmonary veins modulate sinoatrial node pacemaker function. *Cardiovasc Res* 99: 566-575, 2013.
46. **Zhu SH, Sun JY, Bonnevie E, Cummins SE, Gamst A, Yin L, and Lee M**. Four hundred and sixty brands of e-cigarettes and counting: implications for product regulation. *Tobacco control* 23 Suppl 3: iii3-9, 2014.

FIGURE LEGENDS

Figure 1: A: Picture of the Smok Species Baby V2 vaping device. The black screen displays the duration of the activation every time the firing button is pressed. B: Vaping chamber design. C: E-vapor extract generation.

Figure 2: Quantification of Annexin V staining in HL-1 cells with flow cytometry. A: Flow cytometry analysis of live, apoptotic, and necrotic HL-1 cells cultured for 48 h with 0.75 puffs/ml air, or 0.75 puffs/ml vanilla custard (VC) e-vapor extract. B,C,D: Flow cytometry quantification of the percentage of live (B), necrotic (C), and apoptotic (D) cells, in air or Vanilla Custard e-vapor bubbled medium at 0.075, 0.15, 0.375 and 0.75 puffs/ml. E. Toxicity index normalized to that of air. N= 3 in each condition. ($^{\#}p<0.05$ vs air, and $*p<0.01$ vs air, t-test)

Figure 3: A: Toxicity of Air, POG, Vanilla Custard (VC), and Apple Jax (APJ) e-liquid vapor extracts at 0.75 puffs/ml, for 48h in HL1 cells using flow cytometry and Annexin V staining. N=3 in each condition. ($^{\#}p<0.05$ and $*p<0.01$ versus air, and $**p<0.01$ vs POG, one way ANOVA, Bonferroni correction). B: GC-MS chromatograms of vanilla custard (VC), apple jax (APJ) and

POG. Propylene glycol, glycerin and nicotine peaks are evident in addition to flavorings peaks corresponding to aldehydes products such as cinnamaldehyde, vanillin and ethyl vanillin (black arrows). The list of identified constituents is in Table 2.

Figure 4: Effects of 24 h, 0.15 puffs/ml e-vapor exposure on beating rate and corrected field potential duration in human iPSC derived cardiomyocytes. Quantification of (A) beating rate and (B) field potential duration (FPD) after 24 h, 0.15 puffs/ml exposure to air control and POG, vanilla custard (VC), and apple jax (APJ) e-vapors (*$p<0.05$ vs air, and $^{\#}p<0.05$ vs VC and APJ, one way ANOVA, Bonferroni correction. N= 4 each). C: Multiple electrodes array (MEA) recordings of extracellular potentials in the spontaneously beating myocytes after 24 h, 0.15 puffs/ml exposure to: air control (trace 1), 70VG/ 30PG base alone (trace 2), 70VG/ 30PG base plus 0.6mg/ml nicotine (trace 3), and VC (trace 4). Trace 5 is 24 h treatment with 0.375 puffs/ml VC. Scale bar= 500 ms. D: Quantification of (D) beating rate and (E) field potential duration (FPD) after 24 h, 0.15 puffs/ml exposure to air control (N=10) and base alone (N=8), base plus 0.6mg/ml nicotine (N=5), and vanilla custard (VC, N=10) e-vapors (*$p<0.05$ vs air, and $^{\#}p<0.05$ vs VC and APJ, one way ANOVA, Bonferroni correction).

Figure 5: Patch clamp measurement of hERG in transfected HEK293 cells exposed to vanilla custard. HEK293 cells were cotransfected with hERG and GFP, and exposed for 24 hours to 0.375 puffs/ml vanilla custard e-vapor. A: Current traces elicited in response to voltage step protocol (10 mV steps from -60 to 60 mV for 3 s, then step to -40 mV for 1 s, and hyperpolarized to –120 mV for 0.5 s) in an air control (top) and a VC exposed cell. B: IV curve of the I_{Kr} tail current from air (n=8) and VC (n=7) exposed cells. *$p<0.05$, t-test.

Figure 6: Assessment of heart rate variability in mice exposed to air or vanilla custard e-vapor. A: Histograms of the successive differences in NN segments in an air control (left) and a vaped

mouse (right) at baseline (blue) and at 10 weeks exposure (prange). B: Temporal parameters SDNN(ms) and pNN06(%) at baseline, 1 week, 5 weeks and 10 weeks exposure to air (black circles, N= 5 animals) or vaping (gray circles, N= 5 animals). C. Periodograms as estimators of the PSD in an air control (left) and a vaped mouse (right) at baseline (blue) and at 10 weeks exposure (orange). D: Spectral parameters LF (nu) and HF (nu) at baseline, 1 week, 5 weeks and 10 weeks exposure to air (black circles, N= 5 animals) or vaping (gray circles, N= 5 animals). *$p<0.05$, t- test, vape versus air at 5 weeks, and $^{\#}p<0.05$, t- test, vape versus air at 10 weeks.

Figure 7: In- vivo inducibility of VT in mice exposed to air or vanilla custard e-vapor. ECG traces of inducible VT in air control (top trace) and vaped (bottom trace) mice are shown. The bar graph compiles the duration of inducible VT episodes in 6 out of 7 control and 5 out of 5 vaped mice (*$p<0.05$, t-test). Stim: Burst pacing stimulation.

Figure 8: Optical mapping in isolated Langendorff- perfused mouse hearts. A and B: First (beat 1) and second (beat 2) rows: APD_{75} maps of 2 consecutive beats in pacing at 10 (A) and 15 Hz (B). Single pixel optical action potential traces are shown. Third row: difference maps of APD_{75} maps of beats 1 minus beat 2. C and D: Average APD_{75} at different pacing frequencies (8 to 15 Hz) in air control (C, N=4) and VC exposed (D, N=3) mice. *$p<0.05$, t-test. RV; right ventricle. LV; left ventricle. White step symbol: pacing site.

Table 1: GC-MS settings used for qualitative analysis of the e-vapors.

Instrument parameters	
Column	HP-5MS UI (30m x 0.250 mm x 0.25µm)
Carrier gas flow	He @ 1.00 mL/ min (constant flow)
Inlet temperature	250°C
Oven program	Ramp 1: 40°C to 170°C @ 10°C/min; hold 2 min; Ramp 2: 8°C/min to 250°C; Ramp 3: 25°C/min to 320°C; hold 5 min.
Injection volume	250 µL, split (20:1)
Transfer Line temperature	290°C
MS source	Single quadrupole, EI @ 250°C
Solvent delay	1.00 min
MS acquisition range	30-450 amu from 1 min to 32.80 min

Retention Time (RT)	Constituents [a]	Retention Index [a,b] (RI)	Vanilla Custard	Apple Jax	POG

Table 2: GC-MS peaks analysis of the e-vapors.

2.392	Acetoin	713	✓		
2.961	Propylene Glycol	740	✓	✓	✓
3.59	3-Hexenol	857			✓
3.633	Butanoic acid, ethyl ester	802	✓		
4.32	Butanoic acid, 3-methyl-, ethyl ester	854		✓	
6.005	Glycerin	-	✓	✓	✓
6.102	Piperazine	-		✓	
6.915	Cyclotene	1034	✓		
6.988	Benzyl alcohol	1036		✓	
7.183	Furaneol	1070			✓
7.762	D-Limonene	-			✓
7.908	Phenol, 2-methoxy	1090	✓		
8.127	Butanoic acid, 3-methyl-, 3-methylbutyl ester	1104	✓		
8.254	Maltol	1110		✓	✓
9.038	Benzene, 1,4-dimethoxy	1168	✓		
9.593	Ethyl maltol	1199	✓	✓	
10.401	Benzaldehyde, 4-methoxy	1251	✓		
10.625	Cinnamaldehyde	1270		✓	
10.703	Sulfurol	1288	✓		
10.776	Anisyl alcohol	1290	✓		
11.725	Pyridine	1361	✓	✓	✓
11.881	2(3H)-Furanone, dihydro-5-pentyl-	1363	✓		
12.105	2-Propenoic acid	-		✓	
12.154	Cinnamic acid, methyl ester	1379			✓
12.397	Vanillin	1404	✓	✓	
12.942	Coumarin	1441		✓	
13.118	Ethyl Vanillin	1453	✓	✓	
13.244	2(3H)-Furanone, 5-hexyldihydro-	1470		✓	✓
16.691	Vanillin propylene glycol acetal	1686	✓	✓	

"a" NIST 2017 MS database. "b" Semi-standard nonpolar value.

Figure 1:

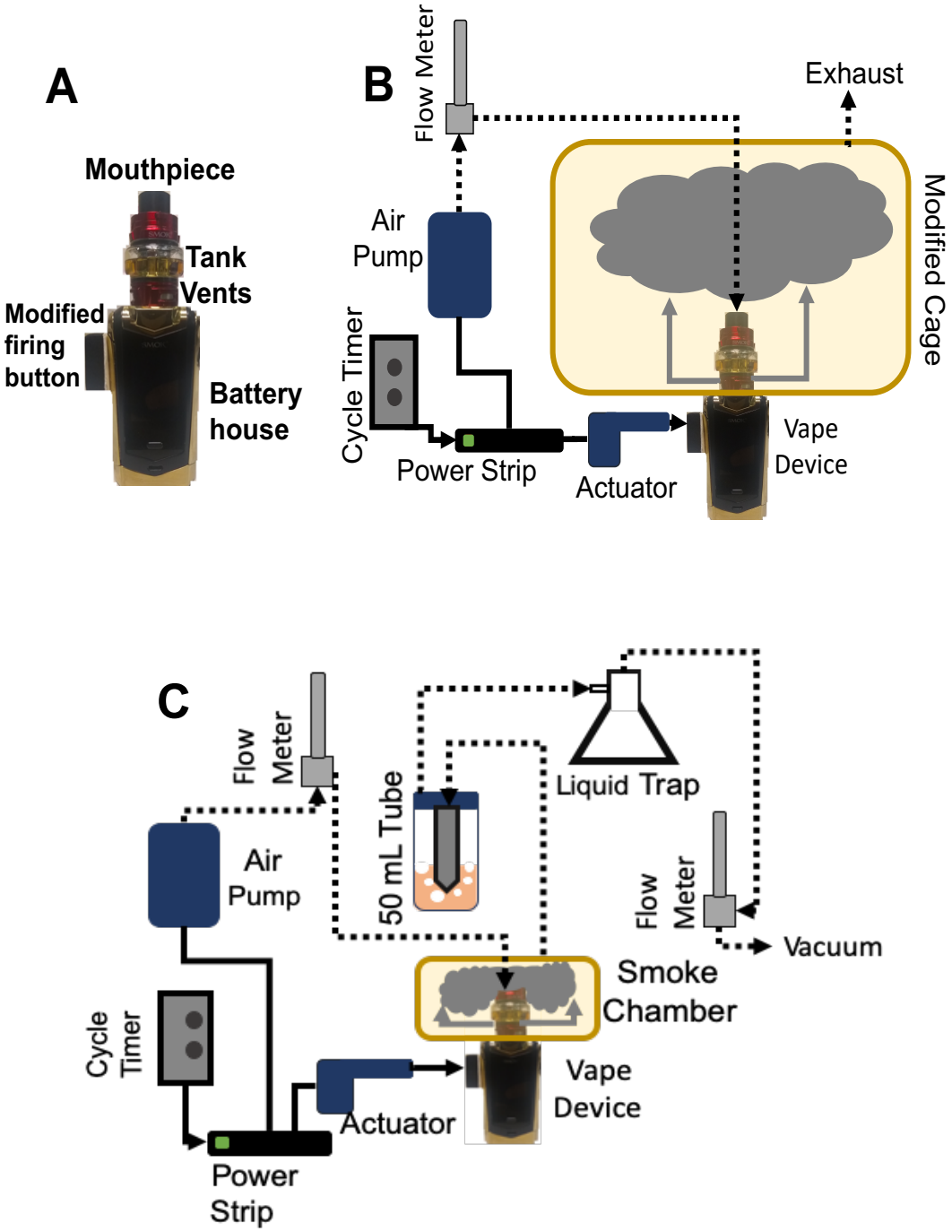
A
Mouthpiece
Tank Vents
Modified firing button
Battery house
B
Flow Meter
Exhaust
Air Pump
Modified Cage
Cycle Timer
Power Strip
Actuator
Vape Device
C
Flow Meter
Liquid Trap
50 mL Tube
Air Pump
Flow Meter
Vacuum
Smoke Chamber
Cycle Timer
Vape Device
Actuator
Power Strip

Figure 2:

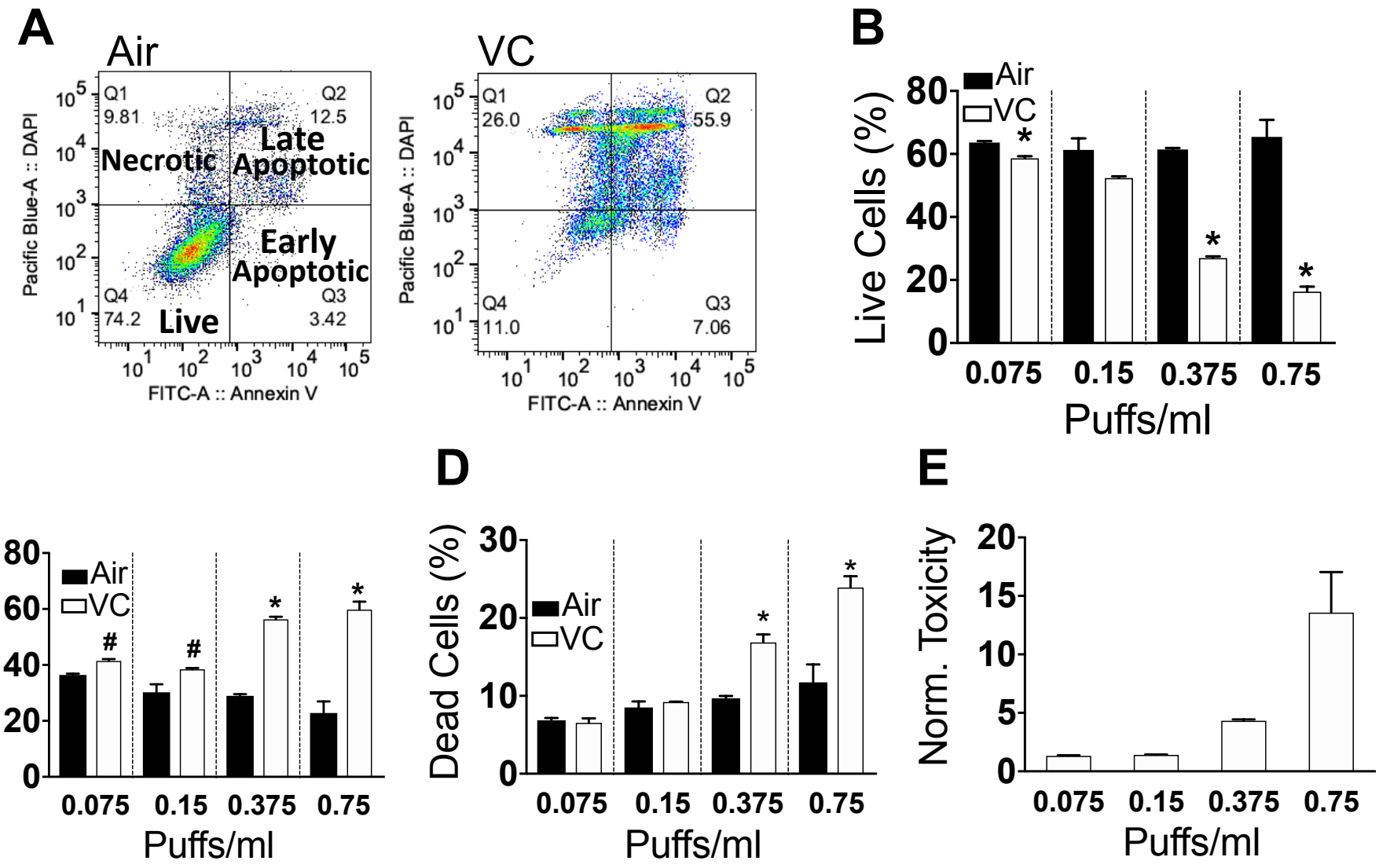
A
Air
VC
Q1
9.81
Q2
12.5
Necrotic
Late Apoptotic
Early Apoptotic
Q4
74.2
Live
Q3
3.42
Pacific Blue-A :: DAPI
FITC-A :: Annexin V
Q1
26.0
Q2
55.9
Q4
11.0
Q3
7.06
B
Air
VC
Live Cells (%)
Puffs/ml
0.075
0.15
0.375
0.75
C
Apoptotic Cells (%)
D
Dead Cells (%)
E
Norm. Toxicity

Figure 3:

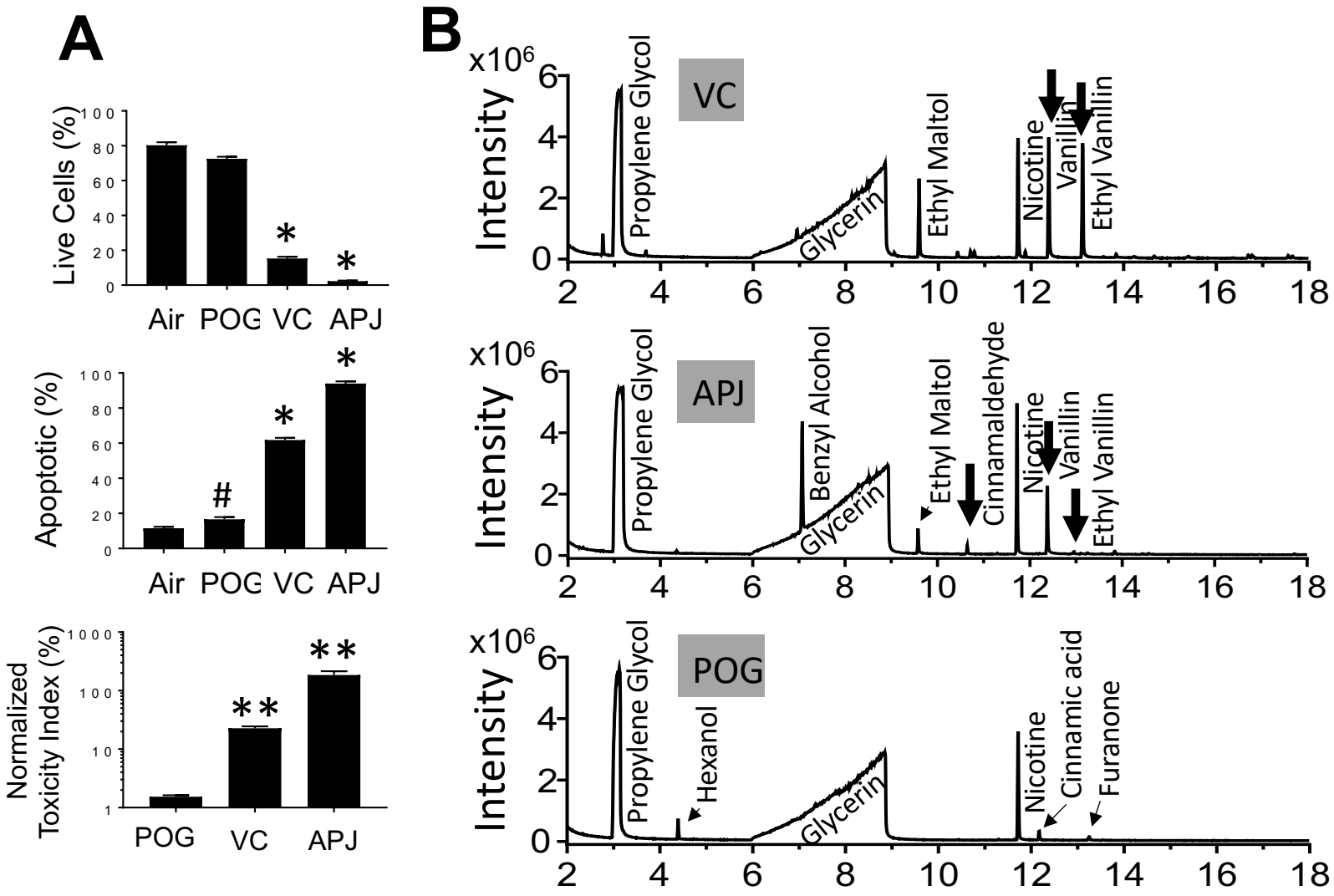
A
Live Cells (%)
100
80
60
40
20
0
*
*
Air POG VC APJ
Apoptotic (%)
100
80
60
40
20
0
#
*
*
Air POG VC APJ
Normalized Toxicity Index (%)
1000
100
10
1
**
**
POG VC APJ
B
x10^6
Intensity
6
4
2
0
VC
Propylene Glycol
Glycerin
Ethyl Maltol
Nicotine
Vanillin
Ethyl Vanillin
2 4 6 8 10 12 14 16 18
APJ
Propylene Glycol
Benzyl Alcohol
Glycerin
Ethyl Maltol
Cinnamaldehyde
Nicotine
Vanillin
Ethyl Vanillin
POG
Propylene Glycol
Hexanol
Glycerin
Nicotine
Cinnamic acid
Furanone

Figure 4:

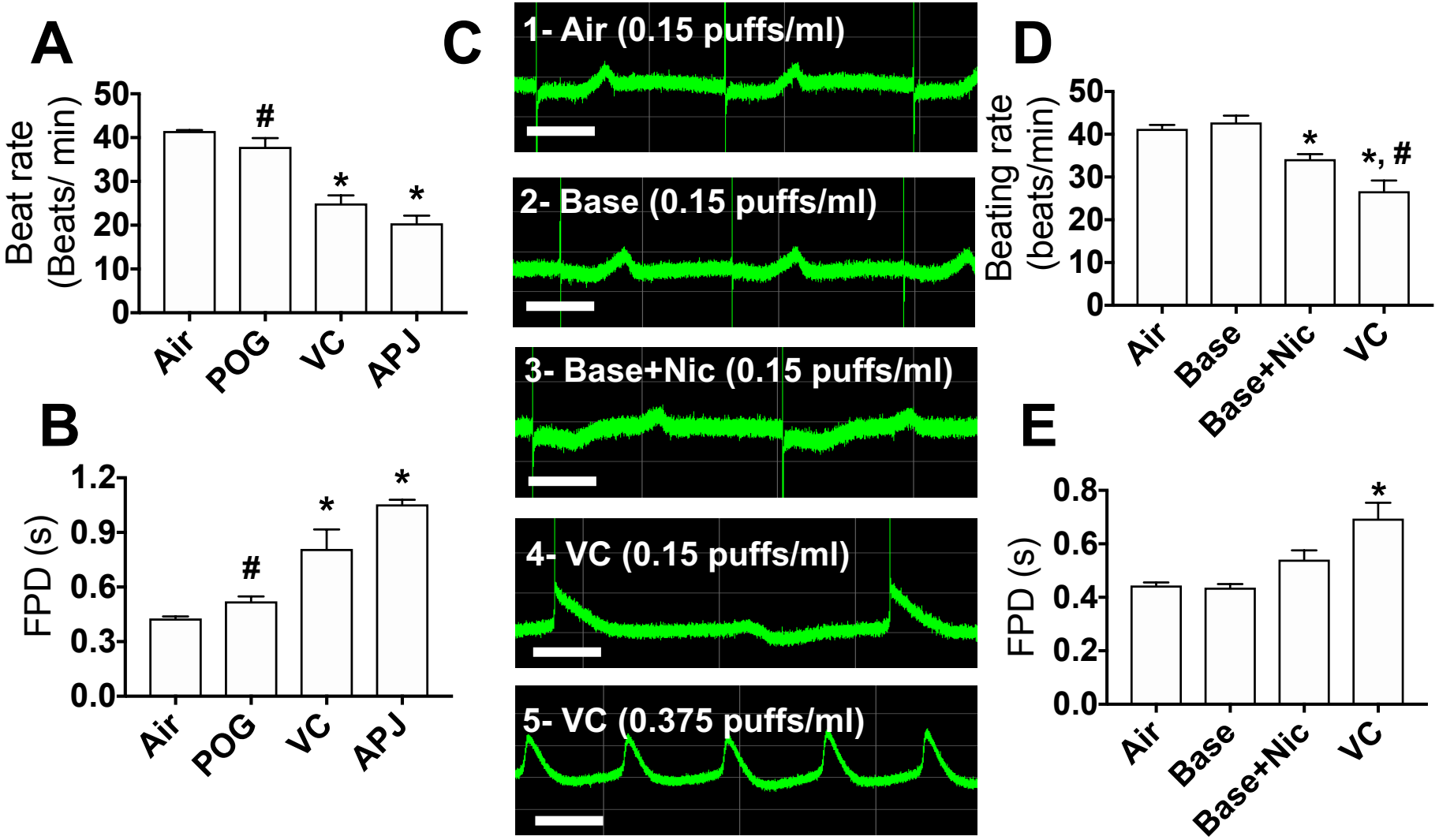
A
Beat rate (Beats/ min)
50
40
30
20
10
0
#
*
*
Air
POG
VC
APJ
B
FPD (s)
1.2
0.9
0.6
0.3
0.0
#
*
*
Air
POG
VC
APJ
C
1- Air (0.15 puffs/ml)
2- Base (0.15 puffs/ml)
3- Base+Nic (0.15 puffs/ml)
4- VC (0.15 puffs/ml)
5- VC (0.375 puffs/ml)
D
Beating rate (beats/min)
50
40
30
20
10
0
*
*, #
Air
Base
Base+Nic
VC
E
FPD (s)
0.8
0.6
0.4
0.2
0.0
*
Air
Base
Base+Nic
VC

Figure 5:

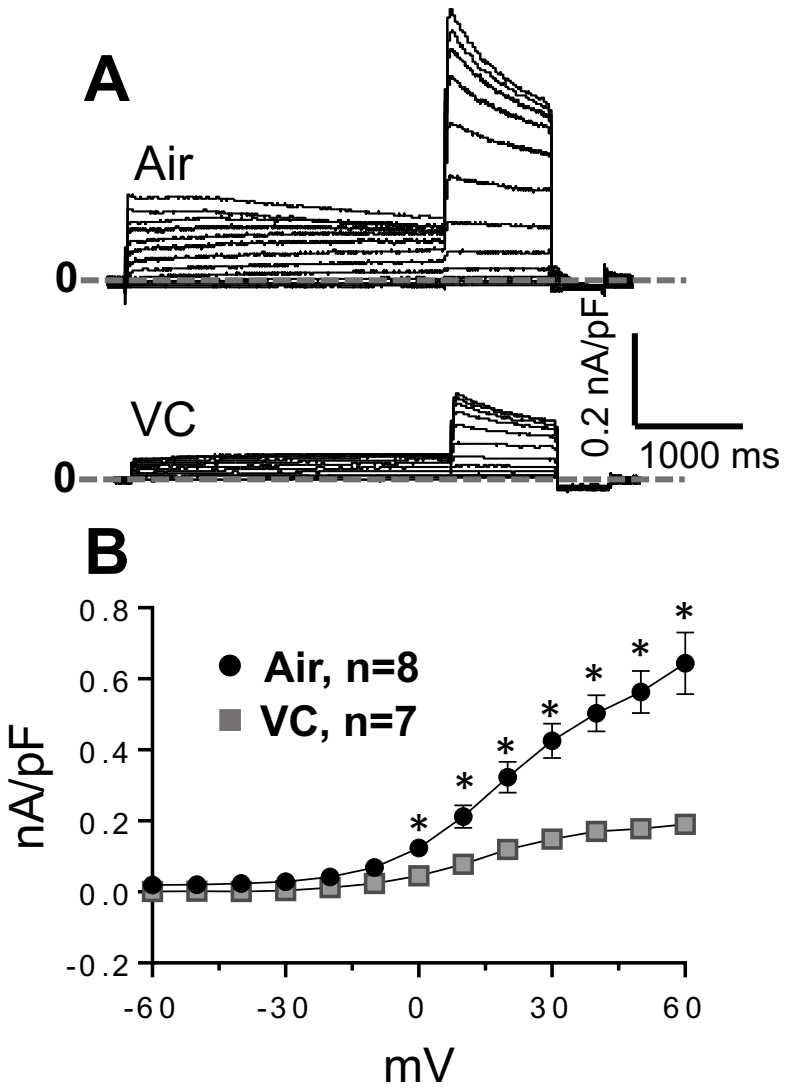
A
Air
0
VC
0
0.2 nA/pF
1000 ms
B
Air, n=8
VC, n=7
nA/pF
0.8
0.6
0.4
0.2
0.0
-0.2
-60
-30
0
30
60
mV
*

Figure 6:

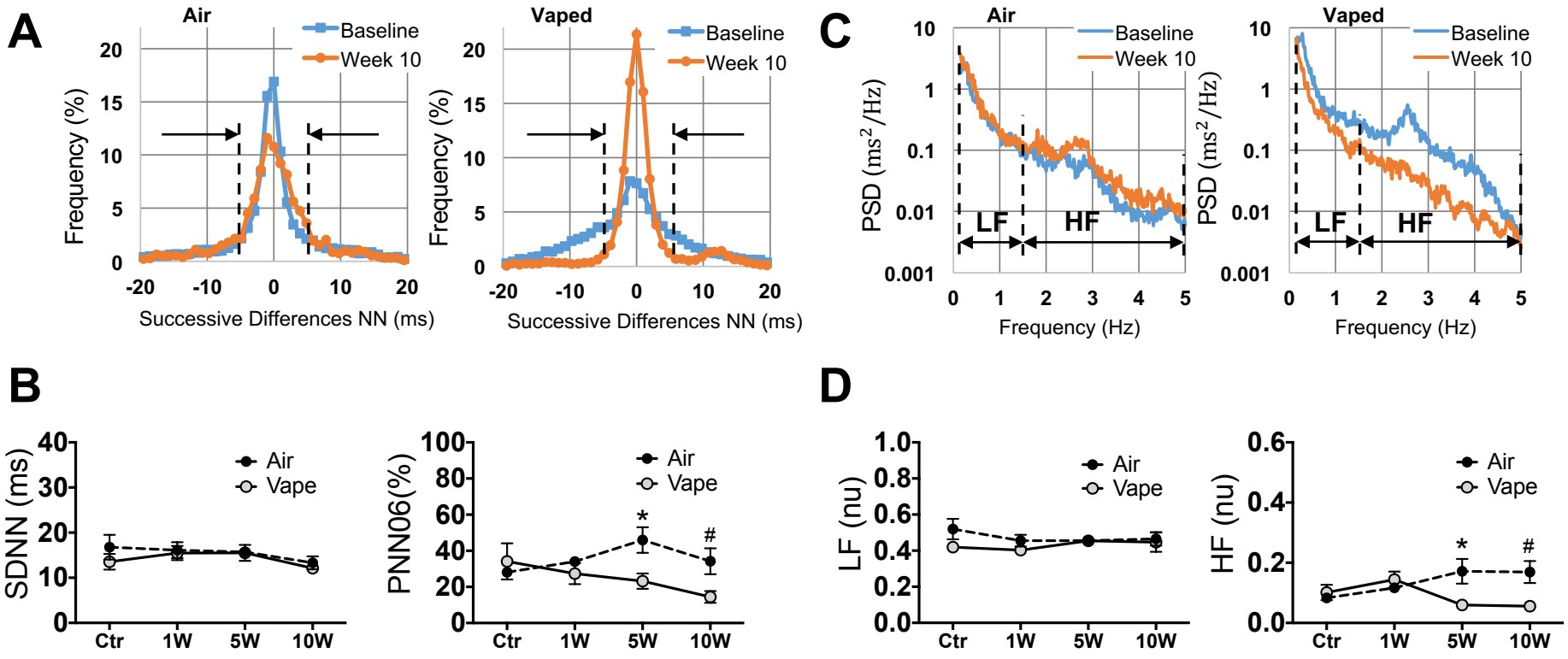
A
Air
Baseline
Week 10
Frequency (%)
Successive Differences NN (ms)
Vaped
C
PSD (ms²/Hz)
LF
HF
Frequency (Hz)
B
SDNN (ms)
Air
Vape
Ctr
1W
5W
10W
PNN06(%)
*
#
D
LF (nu)
HF (nu)

Figure 7:

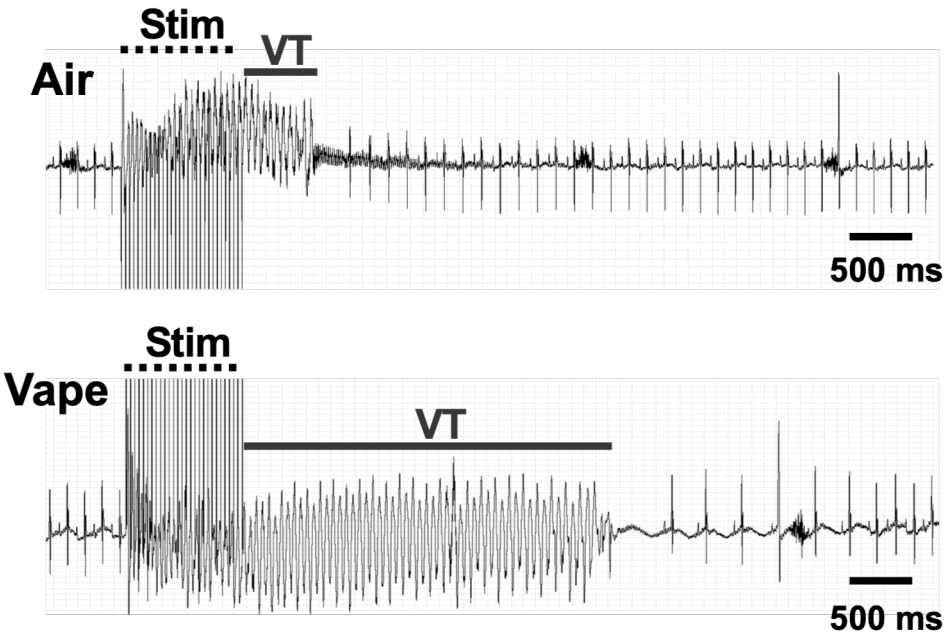
Stim
VT
Air
500 ms
Stim
Vape
VT
500 ms

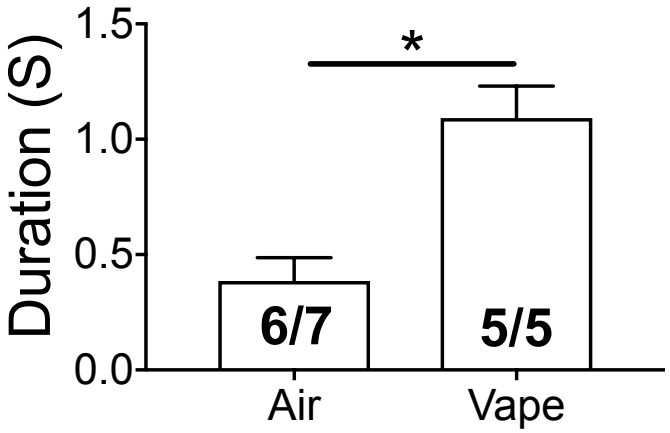
Duration (S)
1.5
1.0
0.5
0.0
*
6/7
5/5
Air
Vape

Figure 8:

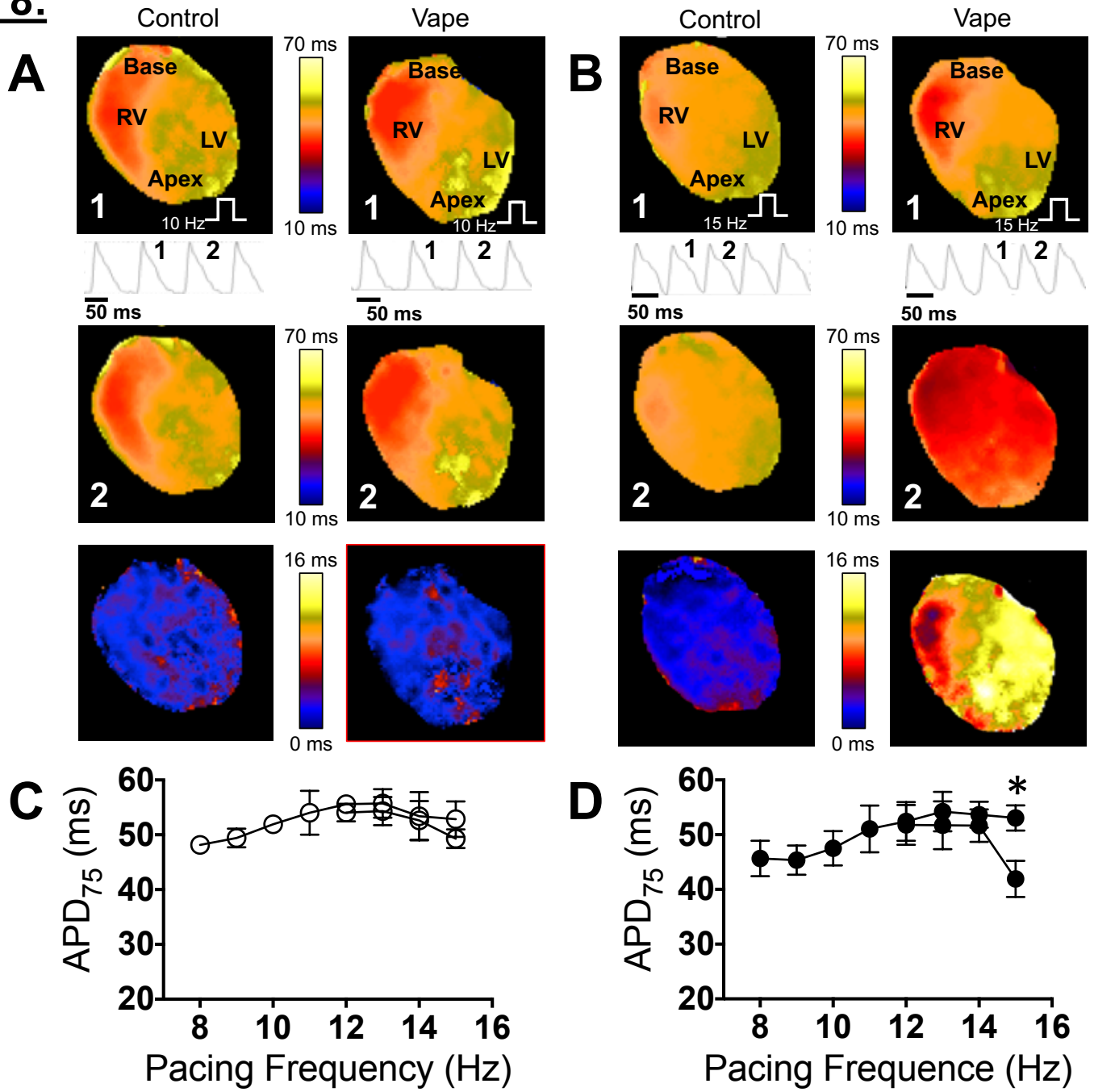
A
Control
Vape
Base
RV
LV
Apex
1
10 Hz
70 ms
10 ms
1
2
50 ms
2
16 ms
0 ms
B
15 Hz
C
APD_{75} (ms)
Pacing Frequency (Hz)
D
*
Pacing Frequence (Hz)